A Study of Angular Stationarity of 5G Millimeter Wave Channels

Conference Paper · February 2018

CITATION
1

READS
283

4 authors, including:

Yi Tan
Heriot-Watt University
9 PUBLICATIONS **244** CITATIONS
SEE PROFILE

Jie Huang
Southeast University (China)
20 PUBLICATIONS **155** CITATIONS
SEE PROFILE

A Study of Angular Stationarity of 5G Millimeter Wave Channels

Yi Tan[1], Jie Huang[2], Rui Feng[2], and Cheng-Xiang Wang[1]
[1]Institute of Sensors, Signals and Systems, School of Engineering & Physical Sciences, Heriot-Watt University, Edinburgh EH14 4AS, UK.
[2]Shandong Provincial Key Lab of Wireless Communication Technologies, Shandong University, Jinan 250100, Shandong, China.
Email: yi.tan@hw.ac.uk, hj_1204@sina.cn, fengxiurui604@163.com, cheng-xiang.wang@hw.ac.uk

***Abstract*—This paper introduces an angular averaged power delay profile (A-APDP) method to determine the angular stationarity region (ASR) of the wireless channels. It is an extension of former studies about the stationarity of channels in time, frequency, and spatial domains. We apply this method to the data of a mmWave channel measurement, and estimate the ASRs of channel based on the directional channel impulse responses (D-CIRs) in different azimuth angles. We also estimate the root mean square (RMS) delay spreads (DSs) and K-factors based on corresponding D-CIRs. Aligning all the results in azimuth angles, we find that the D-CIRs can be sorted into three types. This relates to the existence of light-of-sight (LOS) component and the situation of non-LOS (NLOS) components observed from the D-CIRs.**

***Index Terms*—mmWave channels, directional channel impulse response, angular averaged power delay profile method, angular stationarity region.**

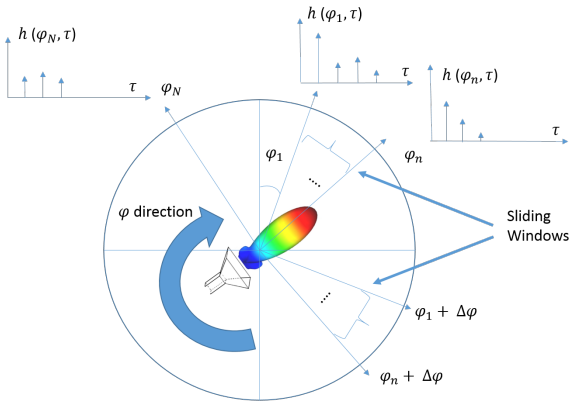

Fig. 1. A-APDP method based on angular sliding windows.

I. Introduction

Due to the very high attenuation of mmWave signals, beamforming is an enabling technology for 5G mmWave communications [1]. It is typical that both the transmitter (Tx) and receiver (Rx) are casting beams that are aligned to each other for data transmission. In this case, the mmWave signals propagate along only one direction from the Tx to Rx, which is different from the omni-directional propagation of the transmitted signals in former wireless communication systems. In the system level analysis, for each instance of mmWave signal transmission, we should have the directional knowledge of the wireless channels.

From the channel measurements in [2], [3], the data showed that the amplitudes and delays of the multipath components (MPCs) estimated from different D-CIRs measured by horn antenna are quite different. In order to address the multipath parameters for both omni-directional and directional channels, a statistical mmWave channel model has been developed in [4] with separate temporal and spatial statistical descriptions of the mmWave channels. The efforts made in this model enable us to observe the directionality of mmWave channels in system level simulations.

However, the directional knowledge of mmWave channels should to be further analyzed. The stationarity of mmWave channels in angular domain needs to be addressed. This paper proposes an A-APDP method to determine the ASR of the mmWave channels, it could help to clarify our understanding of the channel properties in different directions. The study about the ASRs of channels are very useful in both the parameter estimations based on mmWave channel measurements and the mmWave channel modeling.

The rest of this paper is organized as follows. Section II introduces an A-APDP method to study the stationarity of channel in angular domain. Section III presents a mmWave channel measurement, and the D-CIRs are measured by horn antenna pointing to different azimuth angles. In Section IV, the ASRs of mmWave channel are estimated by the A-APDP method, and the condense parameters are estimated as well for the data analysis. Conclusions are finally drawn in Section V.

II. Angular Stationarity

A general APDP method was proposed in [5]. It is used as a metric to determine the stationarity regions of channels in time, frequency, and spatial domains. This method is an extension of the former studies about the stationarity of channels in time and spatial domains [6]. However, the general APDP method could be further extended to angular domain, i.e. A-APDP method, which is described as follows.

For a beam aligned directional wireless channel between the Tx and Rx, we define $h(\phi_i, \tau)$ as a D-CIR measured by Rx at azimuth angle $\phi_i, i = 1, 2...n$, τ is the excess delay. Then, the instantaneous power delay profile (PDP) is defined

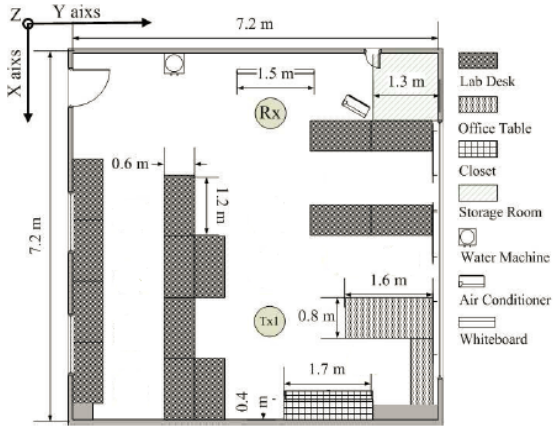

Fig. 2. Layout of an indoor office environment in Shandong University [7].

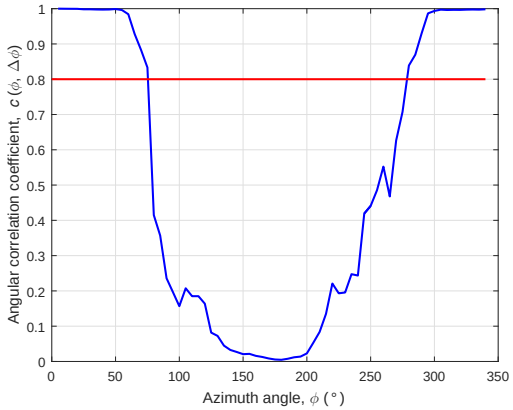

Fig. 3. Angular correlation coefficients between the APDP at azimuth angle $\phi = 0°$ and the APDPs at other azimuth angles.

as $P_h(\phi_i, \tau) = |h(\phi_i, \tau)|^2$ correspondingly. Assume that there are N D-CIRs in total as in Fig. 1, we define $\overline{P_h}(\phi, \tau)$ as

$$\overline{P_h}(\phi, \tau) = \frac{1}{n} \sum_{i=1}^{n} |h(\phi_i, \tau)|^2 \tag{1}$$

to present the APDP of n D-CIRs ($n \ll N$) in one sliding window on azimuth axis ϕ, and we define another APDP $\overline{P_h}(\phi + \triangle\phi, \tau)$ of n D-CIRs in the sliding window as it moves along the azimuth axis ϕ with a distance of $\triangle\phi$. The angular correlation coefficient between the two APDPs is defined as

$$c(\phi, \triangle\phi) = \frac{\int \overline{P_h}(\phi, \tau)\overline{P_h}(\phi + \triangle\phi, \tau)d\tau}{\max\{\int \overline{P_h}(\phi, \tau)^2 d\tau, \int \overline{P_h}(\phi + \triangle\phi, \tau)^2 d\tau\}} \tag{2}$$

and d_ϕ determines the angular stationary interval as the ASR, if the angular correlation coefficients $c(\phi, \triangle\phi)$ between the APDPs are all higher than the allowance of similarity level (ASL) [5], i.e.

$$d_\phi = \max\{\triangle\phi \mid c(\phi, \triangle\phi) \geq c_{\text{ASL}}\}. \tag{3}$$

The n D-CIRs used to calculate the APDPs are in a very small interval that we assume is much smaller than the angular stationary interval. Using the larger value of $\int \overline{P_h}(\phi, \tau)^2 d\tau$ and $\int \overline{P_h}(\phi + \triangle\phi, \tau)^2 d\tau$ in the denominator of (2) is to assure the correlation coefficient is smaller than 1. Note that $\triangle\phi$ can be both positive and negative.

III. Channel Measurement

The indoor mmWave channel measurement was conducted in Shandong University, China, an static office environment as depicted in Fig. 2. In this measurement, Keysight N5227A vector network analyzer (VNA) and Keysight E8257D signal generator were used [7]. The intermediate frequency (IF) filter bandwidth of VNA is 1 kHz and the output power of the signal generator is 13 dBm. The measured frequency range is from 59 to 61 GHz with 401 frequency points (0.5 ns delay resolution). The standard horn antennas with 25 dBi gain and 3-dB beamwidth of 10° at 60 GHz were used in both Tx and Rx. The Tx antenna was placed on the antenna positioner at Tx1 position, and rotated from 0° to 355° in azimuth angle with the step of 5° for each D-CIR measurement (72 D-CIRs in total). While the horn antenna at Rx was hold still pointing to Tx all the time. The heights of Tx and Rx antennas were both 1.6 m.

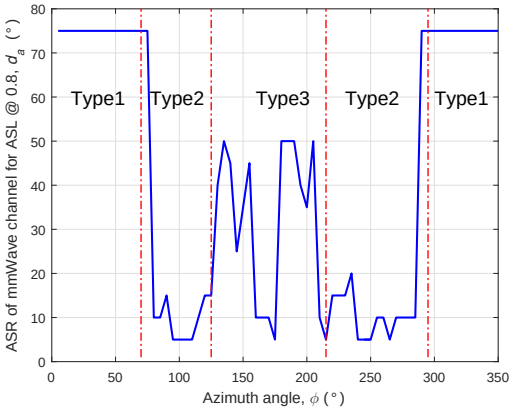

Fig. 4. Estimated ASRs of mmWave channel from D-CIRs in different azimuth angles, ASL is 0.8.

IV. Data Analysis

We apply the A-APDP method to the data of aforementioned mmWave channel measurement, and the angular sliding windows contain three D-CIRs in all the estimations of the ASRs of mmWave channel.

The angular correlation coefficients between the APDP at azimuth angle $\phi = 0°$ and the APDPs at other azimuth angles are shown in Fig. 3. We assume ASL is 0.8, and the estimated ASR of channel at $\phi = 0°$ is about 75°. We have also estimated all the ASRs of channel based on the D-CIRs at different azimuth angles as in Fig. 4. We choose ASL as 0.8 as well, and we can observe that the ASRs of such mmWave channel are in the range from 5° to 75°. The difference could due to the D-CIRs measured in different azimuth angles are impacted by the different propagation situations of the channel.

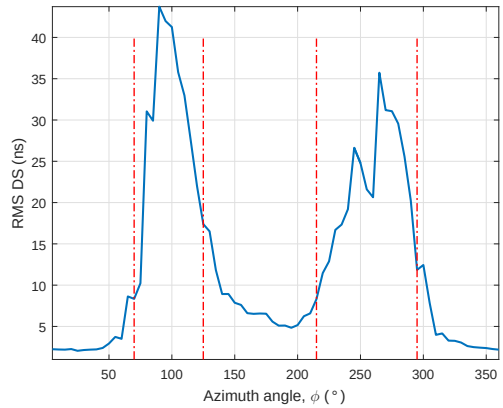

Fig. 5. RMS DS estimated by D-CIRs in azimuth angles.

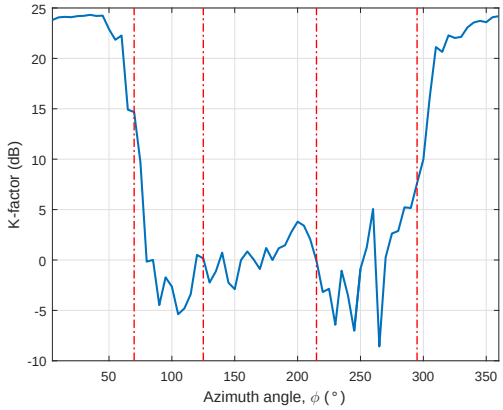

Fig. 6. K-factors estimated by D-CIRs in azimuth angles.

In further analysis, we estimate the condense parameters of channel based on the D-CIRs as well, i.e. RMS DSs and K-factors [8] as in Fig. 5 and Fig. 6. Those could reflect the different propagation situations of the directional mmWave channels in different azimuth angles, such as the existence of the LOS path between Tx and Rx, the power gains of NLOS paths, etc.

Aligning the results in Fig. 4, 5 and 6, we can observe that there exist three types of D-CIRs:

- Type 1: D-CIRs measured at the azimuth angles smaller than $70°$ and larger than $295°$
- Type 2: D-CIRs measured at the azimuth angles between $70°$ and $125°$ & between $215°$ and $295°$
- Type 3: D-CIRs measured at the azimuth angles between $125°$ and $215°$

It is obvious that, the estimated condense parameters are quite similar from the D-CIRs of Type 1 (without the transition area around the borders), which reflects the statistical properties of mmWave channel over two large ASRs (start with azimuth angle $\phi = 0°$ in positive and negative directions). Those estimated condense parameters from the D-CIRs of Type 2 and Type 3 are fluctuating, which reflects the statistical properties

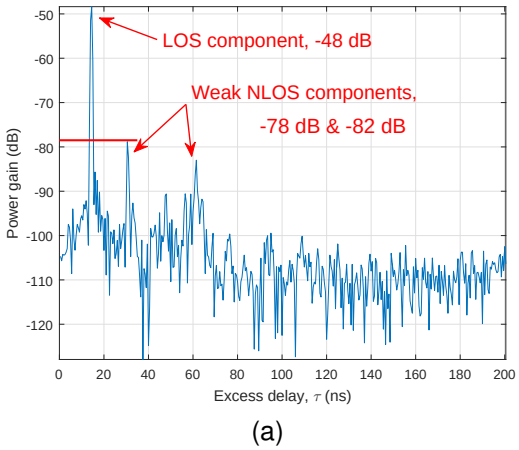

(a)

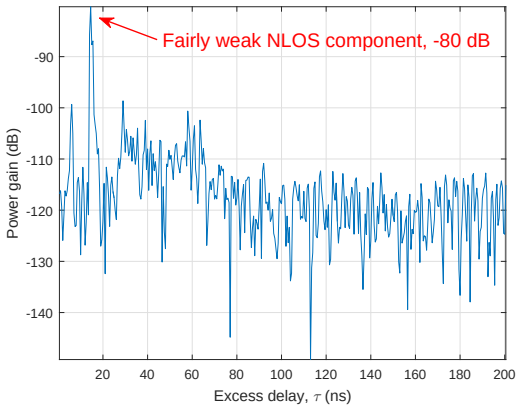

(b)

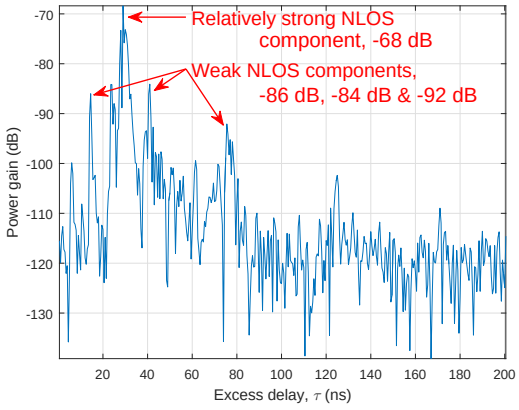

(c)

Fig. 7. Three typical D-CIRs: (a) D-CIR of Type 1, (b) D-CIR of Type 2, and (c) D-CIR of Type 3.

of mmWave channel over a few small ASRs. The ASRs of channel within the azimuth angle coverage of Type 3 D-CIRs are generally larger than those within the azimuth angle coverage of Type 2 D-CIRs.

We plot the typical D-CIRs for each type in Fig. 7. We found that the D-CIRs of Type 1 normally contain one strong LOS

component and two weak NLOS components. They account for high K-factors and small RMS DSs. Those in Type 2 normally contain one fairly week NLOS component, which doesn't have significant high power above the noise floor. This could explain the very low K-factors (mostly below 0 dB) and the dramatically changed RMS DSs in the range between 8.3 and 43.7 ns. Those in Type 3 normally contain one relatively strong NLOS component and a few weak NLOS components. They account for the low K-factors between -2.8 and 3.8 dB, and the RMS DSs change in the range from 4.8 to 17.4 ns.

V. Conclusions

An A-APDP method has been introduced to determine the stationarity region of channel in angular domain. It is an extension of the former general APDP method, which determines the stationarity region of channel in time, frequency, and spatial domains.

In the data analysis of a mmWave channel measurement, we have estimated the ASRs of the channel, RMS DSs, and K-factors based on the D-CIRs measured by horn antenna in different azimuth angles. We have found that, by aligning those results in azimuth angles, we can sort the D-CIRs into 3 types. This relates to the existence of LOS component and the situation of NLOS components observed from the D-CIRs.

Acknowledgment

The authors would like to gratefully acknowledge the support of this work from the EU H2020 ITN 5G Wireless project (Grant No. 641985), the EU H2020 RISE TESTBED project (Grant No. 734325), the EU FP7 QUICK project (Grant No. PIRSES-GA-2013-612652), and the EPSRC TOUCAN project (Grant No. EP/L020009/1).

References

[1] W. Roh, J. Y. Seol, J. Park, B. Lee, J. Lee, Y. Kim, J. Cho, K. Cheun, and F. Aryanfar, "Millimeter-wave beamforming as an enabling technology for 5G cellular communications: theoretical feasibility and prototype results," *IEEE Commun. Mag.*, vol. 52, no. 2, pp. 106–113, Feb. 2014.

[2] T. S. Rappaport, S. Sun, R. Mayzus, H. Zhao, Y. Azar, K. Wang, G. N. Wong, J. K. Schulz, M. Samimi, and F. Gutierrez, "Millimeter wave mobile communications for 5G cellular: It will work!" *IEEE Access*, vol. 1, pp. 335–349, May 2013.

[3] T. S. Rappaport, G. R. MacCartney, M. K. Samini, and S. Sun, "Wideband millimeter-wave propagation measurements and channel models for future wireless communication system design," *IEEE Trans. Commun.*, vol. 63, no. 9, pp. 3029–3056, Sept. 2015.

[4] M. K. Samimi and T. S. Rappaport, "3-D millimeter-wave statistical channel model for 5G wireless system design," *IEEE Trans. Microw. Theory Techn.*, vol. 64, no. 7, pp. 2207–2225, Jul. 2016.

[5] Y. Tan, C.-X. Wang, J. Ø. Nielsen, and G. F. Pedersen, "Comparison of stationarity regions for wireless channels from 2 GHz to 30 GHz," in *Proc. IWCMC'17*, Invited Paper, Valencia, Spain, Jun. 2017, accepted for publication.

[6] A. Gehring, M. Steinbauer, I. Gaspard, and M. Grigat, "Empirical channel stationarity in urban environments," in *Proc. EPMCC'01*, Vienna, Austria, Feb. 2001.

[7] X. Wu, C. X. Wang, J. Sun, J. Huang, R. Feng, Y. Yang, and X. Ge, "60-GHz millimeter-wave channel measurements and modeling for indoor office environments," *IEEE Trans. Antennas Propag.*, vol. 65, no. 4, pp. 1912–1924, Apr. 2017.

[8] A. F. Molisch, *Wireless Communications, Second Edition*. John Wiley & Sons, 2011.